HANSER

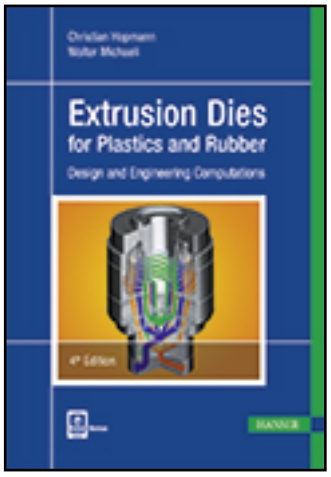

Sample Pages

Christian Hopmann, Walter Michaeli

Extrusion Dies for Plastics and Rubber

Design and Engineering Computations

Book ISBN: 978-1-56990-623-1

eBook ISBN: 978-1-56990-624-8

For further information and order see

http://www.hanser-fachbuch.de/978-1-56990-623-1

or contact your bookseller.

Hopmann, Michaeli
Extrusion Dies for Plastics and Rubber

Christian Hopmann
Walter Michaeli

Extrusion Dies for Plastics and Rubber

Design and Engineering Computations

4th Edition

With Contributions by

Dr.-Ing. Ulrich Dombrowski • Dr. Ulrich Hüsgen • Dr.-Ing. Matthias Kalwa • Dr.-Ing. Stefan Kaul • Dr.-Ing. Michael Meier-Kaiser • Dr.-Ing. Boris Rotter • Dr.-Ing. Micha Scharf • Dr.-Ing. Claus Schwenzer • Dr.-Ing. Christian Windeck • Nafi Yesildag, M.Sc.

HANSER

Hanser Publishers, Munich

Hanser Publications, Cincinnati

The Authors:

Prof. Dr.-Ing. Christian Hopmann,
Head of the Institute of Plastics Processing (IKV) at RWTH Aachen University, Aachen, Germany

Prof. Dr.-Ing. Dr.-Ing. E.h. Walter Michaeli,
former Head of the Institute of Plastics Processing (IKV) at RWTH Aachen University, Aachen, Germany

Distributed in the Americas by:
Hanser Publications
6915 Valley Avenue, Cincinnati, Ohio 45244-3029, USA
Fax: (513) 527-8801
Phone: (513) 527-8977
www.hanserpublications.com

Distributed in all other countries by:
Carl Hanser Verlag
Postfach 86 04 20, 81631 München, Germany
Fax: +49 (89) 98 48 09
www.hanser-fachbuch.de

Cataloging-in-Publication Data is on file with the Library of Congress

Editor: Mark Smith
Production Management: Jörg Strohbach
Coverconcept: Marc Müller-Bremer, www.rebranding.de, München
Coverdesign: Stephan Rönigk
Typesetting: Kösel Media GmbH, Krugzell
Printed and bound by Hubert & Co GmbH, Göttingen
Printed in Germany

ISBN: 978-1-56990-623-1
E-Book ISBN: 978-1-56990-624-8

Preface

In January 2003, this book was published in its 3rd edition in English. Since then, an unrelenting demand for the book has been observed, both for the German and English versions. In order to meet this demand, it is our pleasure that Hanser now publishes this 4th edition. With this edition, "Extrusion Dies" has for the first time two editors: In April 2011 Prof. Dr.-Ing. Christian Hopmann succeeded Prof. Dr.-Ing. Dr.-Ing. E. h. Walter Michaeli as holder of the Chair of Plastics Processing and Head of the Institute of Plastics Processing (IKV) at RWTH Aachen University, Aachen, Germany. We are very pleased that this book with its long history with Hanser is continued into the next IKV generation.

This update will continue to help you in your work and life while hopefully also providing pleasure in reading. We have retained the structure of the book, which has proven itself over many years and received much positive resonance from readers.

When we say "we", we particularly refer to *Dr.-Ing. Christian Windeck,* former head of the IKV extrusion department, and his successor *Nafi Yesildag, M.Sc.,* who have critically analyzed, checked, and supplemented the contents, equations, and reference lists. We would like to express our special thanks to both of them.

We further thank *Mark Smith* and *Jörg Strohbach* of Hanser for their support in the publication of our work.

Once again, suggestions obtained from the plastics and rubber industry were taken up and addressed in this fourth edition. We thank all those who provided their suggestions and help. Many research and development efforts of the IKV form the fundament of some of the facts described in this book. Against this background, we thank the Federal Ministry for Economic Affairs and Energy (BMWi), Berlin, for the promotion of many industrial research projects through the German Federation of Industrial Research Associations (AIF e. V.), Cologne, the Deutsche Forschungsgemeinschaft (DFG), Bonn-Bad Godesberg, the Federal Ministry of Education and Research (BMBF), Bonn, and the European Commission, Brussels, with respect to extrusion dies.

Walter Michaeli

Christian Hopmann

Contents

2 Properties of Polymeric Melts

When we choose a theoretical description of the process correlations in the extrusion die and calibration unit for a reliable design of those systems, there are two things in particular to be considered:

- Simplifications and boundary conditions based on the physical models always have to be analyzed critically with regard to the problem at hand.
- Data pertaining to the processed material and that are being entered into the models become of key importance. These are data that characterize flow, deformation, and relaxation behaviors and heat transfer; in other words, its rheological and thermodynamic data [1].

2.1 Rheological Behavior

A general flow is fully described by the law of conservation of mass, impulse, and energy, as well as by the rheological and thermodynamic equations of state. The rheological state equation, often referred to as the material law, describes the correlation between the flow velocity field and the resulting stress field. All the flow properties of the given polymer enter this equation. The description, explanation, and measurement of the flow properties are at the core of the science of deformation and flow called rheology [2].

Rheology will be introduced in this chapter to the extent to which it is needed for the design of extrusion dies. Polymeric melts do not behave as purely viscous liquids; they also exhibit a substantial elasticity. Their properties therefore lie between ideal Newtonian (viscous) fluids and ideal Hookean (elastic) solids. This is referred to as viscoelastic behavior or viscoelasticity. When describing rheological material behavior, a clear distinction is made between purely viscous behavior and the combination of viscous and time-dependent elastic behavior.

2.1.1 Viscous Properties of Melts

During the process of flow as it occurs in extrusion dies, the melt is subjected to shear deformation. This shearing flow is caused by the fact that melts adhere to the die walls. This is called Stokean adhesion. A change in flow velocity through the flow channel area is the result of this, and it is represented by the following equation:

$$\dot{\gamma} = -\frac{\mathrm{d}\upsilon}{\mathrm{d}y}, \tag{2.1}$$

υ Flow velocity
y Direction of shear

During the steady-state shear flow, a shear stress τ occurs between two layers of the fluid at any point. In the simplest case of a *Newtonian fluid,* this shear stress τ is proportional to the shear rate $\dot{\gamma}$:

$$\tau = \eta \cdot \dot{\gamma}. \tag{2.2}$$

The constant of proportionality η is called the dynamic shear viscosity or simply *viscosity.* Its dimension is Pa·s. The viscosity is the measure of the internal resistance to flow in the fluid under shear.

Generally, polymeric melts do not behave in a Newtonian fashion. Their viscosity is not constant but is dependent on the shear rate. In reference to Equation (2.2) valid for Newtonian fluids, this can be expressed in the following manner:

$$\tau = \eta\left(\dot{\gamma}\right) \cdot \dot{\gamma} \tag{2.3}$$

or

$$\eta\left(\dot{\gamma}\right) = \frac{\tau}{\dot{\gamma}} \neq \text{const.} \tag{2.4}$$

Note: Many polymers exhibit more or less pronounced time-dependent viscosity (thixotropy, rheopexy, lag in viscosity at sudden onset of shear or elongation [2,3]). This time dependence is usually not considered in the design of dies; hence it will be ignored in the following sections.

2.1.1.1 Viscosity and Flow Functions

When plotting the viscosity η in dependence on the shear rate $\dot{\gamma}$ in a log-log graph, we obtain a function shown in Fig. 2.1 valid for polymers at constant temperature. It can be seen that for low shear rates the viscosity remains constant; however, with increasing shear rate at a certain point it changes linearly over a relatively broad range of shear rates in a log-log graph.

This, the reduction of viscosity with increased shear rate, is referred to as pseudoplastic or shear-thinning behavior. The constant viscosity at low shear rates is called zero-shear viscosity, η_0.

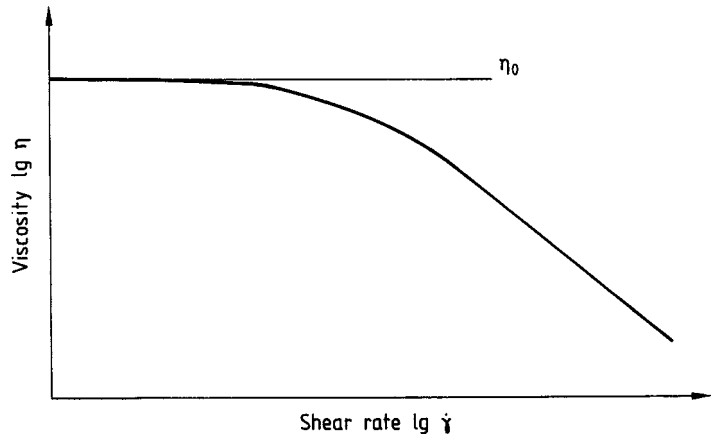

Figure 2.1 Representation of the dependence of viscosity on the shear rate by a viscosity curve

Besides the graphic representation of viscosity vs. shear rate, the so-called *viscosity curve,* the relationship between shear stress and shear rate (also in a log-log graph) is referred to as a *flow curve* (Fig. 2.2). For a Newtonian fluid, the shear rate is directly proportional to the shear stress. A log-log graph therefore is a straight line with a slope of 1, which means that the angle between the abscissa and the flow curve is 45°. Any deviation from this slope directly indicates a non-Newtonian behavior.

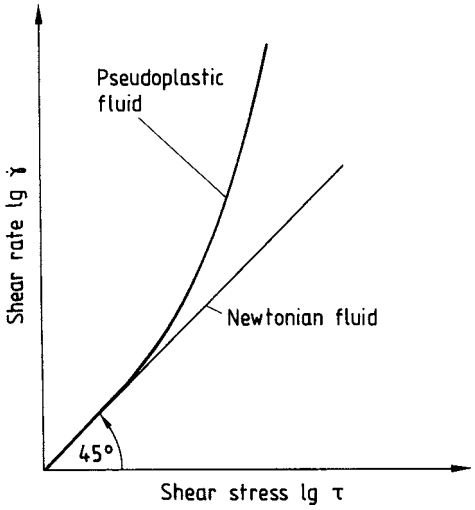

Figure 2.2 Representation of the dependence of the shear rate on the shear stress by a flow curve

For a pseudoplastic fluid, the slope is greater than 1, meaning that the shear rate increases progressively with increasing shear stress. Conversely, the shear stress increases with the shear rate in a less-than-proportional relationship (see also Chapter 3).

2.1.1.2 Mathematical Description of the Pseudoplastic Behavior of Melts

Various models describing the viscosity and flow curves were developed mathematically. They differ in the mathematical methods used on one hand and in the adaptability and hence accuracy on the other. An overview and examples are given in the literature [2,4]. The most widely used models for thermoplastics and rubbers will be discussed in the following section.

***Power Law of Ostwald and de Waele* [5,6]**

When plotting the flow curves of different polymers in a log-log graph, curves are obtained that consist of two approximately linear sections and one transition region (Fig. 2.3). In many cases we can operate in one of those two regions, so these sections of the curve can be mathematically represented in the following general form:

$$\dot{\gamma} = \phi \cdot \tau^{\mathrm{m}} \tag{2.5}$$

Equation (2.5) is called the *power law of Ostwald and de Waele*. The parameters are m, the flow exponent, and ϕ, the fluidity. Characteristic for the ability of a material to flow and its deviation from Newtonian behavior is the flow exponent m. It can be expressed by the following relation:

$$m = \frac{\Delta \lg \dot{\gamma}}{\Delta \lg \tau} \tag{2.6}$$

Note that m is also the slope of the flow curve in the given sections of the log-log diagram (Fig. 2.3).

The value of m for polymeric melts lies between 1 and 6; for the range of shear rates between approximately 10^0 and 10^4 s^{-1} applicable to the design of extrusion dies, the corresponding values of m are between 2 and 4. For $m = 1$, $\phi = 1/\eta$, which is the case of a Newtonian flow.

Since

$$\eta = \frac{\tau}{\dot{\gamma}}$$

we obtain from Equation (2.5):

$$\eta = \phi^{-1} \cdot \tau^{1-\mathrm{m}} = \phi^{-\frac{1}{\mathrm{m}}} \cdot \dot{\gamma}^{\frac{1}{\mathrm{m}}-1}. \tag{2.7}$$

By substituting $k = \phi^{-\frac{1}{\mathrm{m}}}$ and $n = \dfrac{1}{m}$ we obtain the usual representation of the viscosity function:

$$\eta = k \cdot \dot{\gamma}^{\mathrm{n}-1}. \tag{2.8}$$

The factor k is called the consistency factor. It represents the viscosity at a shear rate of $\dot{\gamma} = 1/s$. The viscosity exponent n is equal to 1 for Newtonian behavior, and its value for most polymers is between 0.2 and 0.7. It represents the slope of the viscosity curve in the observed range.

The power law is very simple mathematically: it allows an analytical treatment of almost all simple flow problems that can be solved for Newtonian fluids (see Chapter 3). The disadvantage of the power law is that when the shear rate drops to zero, the viscosity value becomes infinity, and therefore the shear-rate-independent Newtonian region cannot be depicted. Another disadvantage is that the flow exponent m enters into the dimension of the fluidity.

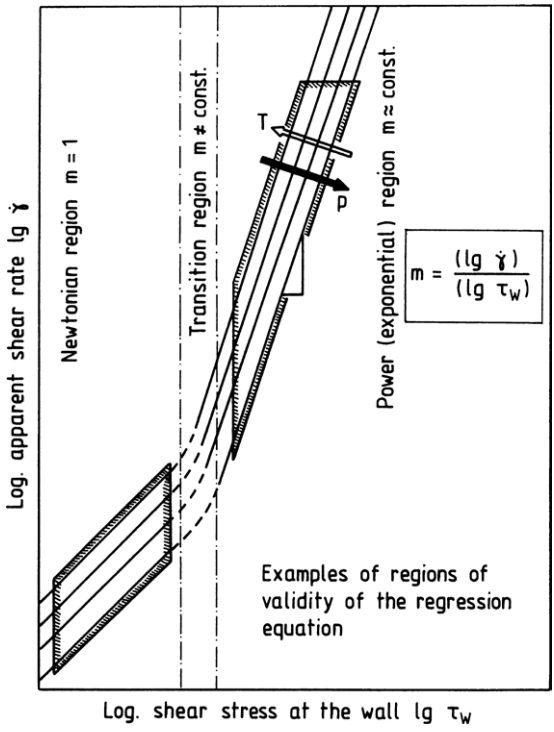

Figure 2.3 Approximation of the flow curve by the power law

Generally, the power law can be used to represent a flow or viscosity curve with an acceptable accuracy over only a certain range of shear rates. The size of this range at a given accuracy depends on the curvature of the graph's representation of this function.

If a flow curve has to be described by the power law over a large range, it has to be divided into segments, each with its own values of ϕ and m to be determined [7]. Therefore, in the collection of standard rheological material data [8,9], there will be different values of ϕ and m corresponding to different ranges of shear rates.

Prandtl-Eyring Constitutive (sinh) Equation [7,10–12]

This model was developed by Prandtl and Eyring from observation of the place-exchange processes of molecules during flow. It takes the following form:

$$\dot{\gamma} = C \cdot \sinh\left(\frac{\tau}{A}\right) \tag{2.9}$$

with material constants C in [s^{-1}] and A in [N/m^2].

The advantage of the Prandtl-Eyring model is that it describes a finite viscosity at small shear rates (zero-shear viscosity) and that it is readily applicable in dimensional analysis [13,14]. Its mathematical application is somewhat difficult, however, because of its unwieldiness.

Carreau Constitutive Equation [9,15,16]

This model, which is gaining increasing importance in the design of extrusion dies, is represented by the following equation:

$$\eta(\dot{\gamma}) = \frac{A}{\left(1 + B \cdot \dot{\gamma}\right)^C} \tag{2.10}$$

where A describes zero-shear viscosity in [Pa·s], B the so-called reciprocal transition rate in [s], and C [–] the slope of the viscosity curve in the pseudoplastic region at $\dot{\gamma} \to \infty$ (Fig. 2.4).

This model by Carreau has an advantage in that it represents the actual behavior of the material over a much broader range of shear rates than the power law, and it produces reasonable viscosity values at $\dot{\gamma} \to 0$.

In addition, it is applicable for the calculation of the correlation between pressure and throughput in a consistent analytical form for both a capillary and a slit die [9,16]. As a result, this model allows rough calculations by means of a pocket calculator. This is particularly useful when a convenient approximate calculation rather than exact analytical solution is required [9,16].

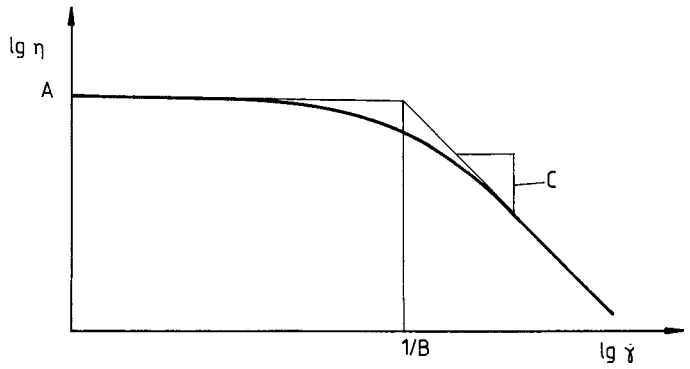

Figure 2.4 Approximation of the viscosity curve by the Carreau constitutive equation

Universal Viscosity Function by Vinogradov and Malkin [17,18]

Vinogradov and Malkin [17] found that, in a temperature-invariant representation (see Section 2.1.1.3), the viscosity functions of the following materials fall within the scatter range shown in Fig. 2.5: polyethylene, polypropylene, polystyrene, polyisobutylene, polyvinylbutyrate, natural rubber, butadiene–styrene rubber, as well as cellulose acetate.

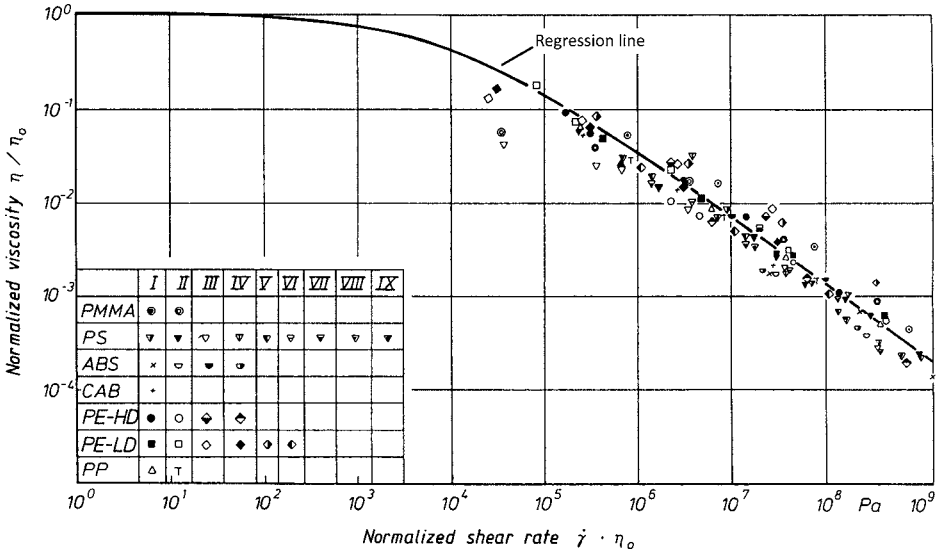

Figure 2.5 Universal viscosity curve according to *Vinogradov* and *Malkin*

The regression line can be considered, at least for the purpose of estimation, to be apparently a universal viscosity function, independent of temperature and pressure. This function allows the estimation of the viscosity behavior over a wide range of shear rates when only one point is known, while the zero-shear viscosity is determined by iteration.

The graphic representation of this universal viscosity function is given by the following regression formula [17]:

$$\eta(\dot{\gamma}) = \frac{\eta_0}{1 + A_1 \cdot (\eta_0 \cdot \dot{\gamma})^{\alpha} + A_2 \cdot (\eta_0 \cdot \dot{\gamma})^{2\alpha}} \tag{2.11}$$

where

η_0 Zero-shear viscosity, i. e., the limiting value of viscosity for $\dot{\gamma} \to 0$

A_1 1.386×10^{-2}

A_2 1.462×10^{-3}

α 0.355

Here, A_1 and A_2 depend on the units of viscosity and shear rate. The values shown here are valid for the following units: $[\eta] = \text{Pa} \cdot \text{s}$ and $[\dot{\gamma}] = \text{s}^{-1}$.

The advantage of the universal Vinogradov function is that it only contains one free parameter, namely zero-shear viscosity η_0, which can be readily determined by the measurements of viscosity. When keeping the regression coefficients A_1, A_2, and α constant, the accuracy of the relation becomes limited. For $\dot{\gamma} \to 0$ the Vinogradov function approaches the limiting value, namely η_0.

In the following section, it will be shown briefly how to calculate, by a simple iteration, the zero-shear viscosity from a measured point $[\dot{\gamma}_p; \eta(\dot{\gamma}_p)]$ with shear rate $\dot{\gamma}_p$ and viscosity $\eta(\dot{\gamma}_p)$. However, the viscosity function obtained by this procedure is only an estimation, and it cannot replace the viscosity measurement in the entire relevant range of shear rates.

The deviations from the actual function are increasing with increasing distance from the known point on the curve $[\dot{\gamma}_p; \eta(\dot{\gamma}_p)]$.

First, the known values are put into Equation (2.11), which is then rearranged as follows:

$$\eta_0 = \eta(\dot{\gamma}_p) \cdot \left[1 + A_1 \cdot (\eta_0 \cdot \dot{\gamma}_p)^{\alpha} + A_2 \cdot (\eta_0 \cdot \dot{\gamma}_p)^{2\alpha}\right]. \tag{2.12}$$

Equation (2.12) contains η_0 on both sides. An explicit solution for η_0 is not possible. Therefore it is subjected to an iteration procedure. It follows

$$\eta_{0_{n+1}} = \eta(\dot{\gamma}_p) \cdot \left[1 + A_1 \cdot (\eta_{0_n} \cdot \dot{\gamma}_p)^{\alpha} + A_2 \cdot (\eta_{0_n} \cdot \dot{\gamma}_p)^{2\alpha}\right]. \tag{2.13}$$

From Equation (2.13) results, with the estimated value of η_{0_n}, an improved estimated value of the zero-shear viscosity $\eta_{0_{n+1}}$ in the *n*th iteration step. The value of $\eta_{0_{n+1}}$ is then put into the $(n+1)$th iteration step using Equation (2.13). The following iteration process results:

Step 0: Set η_{0_0} equal to the known value of viscosity, $\eta(\dot{\gamma}_p)$.

Step 1: Calculate the new estimated value for η_0 by putting the previous estimated value into Equation (2.13).

Step 2: Decision: If the difference of the two subsequent estimated values is small enough, the iteration is stopped. The last estimated value for η_0 is the desired result. If the difference is not small enough, return to step 1

A sufficiently accurate result is usually found after 5 to 10 iterations. The iteration pattern can be easily programmed on a pocket calculator because very few programming steps are required.

Of course, the Vinogradov model in its general form can also be used for the description of the viscosity function. In this case A_1, A_2, and α are free parameters, which can be determined by regression analysis. By this a more accurate approximation is possible than with the parameters of the universal function.

On the other hand, as a universal function defined by the regression line drawn through the data points (Fig. 2.5), any model that approximates the curve with a satisfactory accuracy can be used here instead of Equation (2.11).

Herschel-Bulkley Model [2,12,19]

With many polymers, especially with rubbers, a so-called yield stress is observed. Such fluids start to flow only when a finite shear stress is exceeded (yield stress). Fluids exhibiting this behavior are called Bingham fluids.

The flow curve of a Bingham fluid is shown schematically in Fig. 2.6. It is clearly seen that the shear rate is equal to zero up to the yield stress, τ_0, which means no flow occurs. Only beyond τ_0 will there be flow. This means that the viscosity below the yield stress is infinite [2].

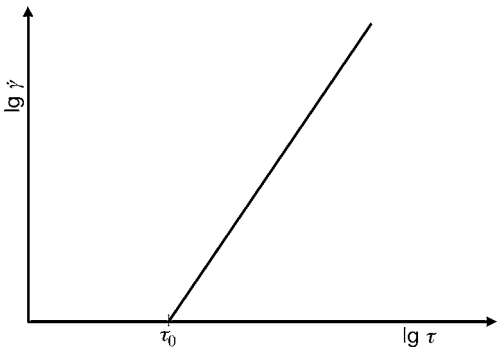

Figure 2.6 Schematic representation of the flow curve of a Bingham fluid

In a developed flow rate profile of a Bingham fluid, there will be one range of shear flow in which the shear stress τ is larger than τ_0 and another one in which τ is smaller than τ_0 (Fig. 2.7 [20]). Figure 2.7 also shows that the proportion of the so-called plug flow diminishes with the increase in the ratio of the shear stress at the wall and the yield stress. Therefore, the plug-shear flow model is valid when the shear stress at the wall is low, that is, when there is a small volumetric flow rate or a large die cross section.

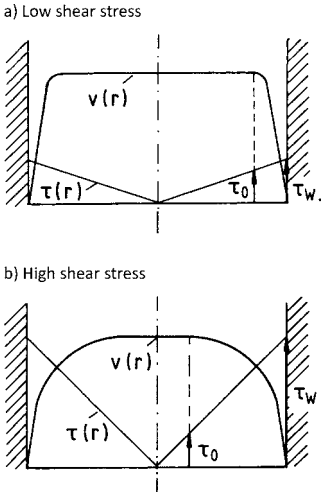

Figure 2.7 Velocity profile of a Bingham fluid in dependence on the shear stress at the wall and the yield stress [20]: (a) low shear stress, (b) high shear stress

The Herschel-Bulkley model [19] has been successful in describing the flow behavior of polymers with a yield stress. This model results from the combination of a simplified Bingham model (with $\eta = \text{const.}$ for $\tau > \tau_0$ [2]) and the power law, yielding

$$\dot{\gamma} = \phi \cdot \left(\tau - \tau_0\right)^{\mathrm{m}}. \tag{2.14}$$

For $\tau_0 = 0$ the relation becomes the power law (Equation (2.5)) and for $m = 1$ the simple Bingham model.

When rearranging Equation (2.14) the following expression for the shear stress is obtained:

$$\tau - \tau_0 = k \cdot \dot{\gamma}^{\mathrm{n}-1} \cdot \dot{\gamma} \tag{2.15}$$

where

$$k = \phi^{-\frac{1}{m}} \quad \text{and} \quad n = \frac{1}{m}.$$

with

$$\eta = \frac{\tau - \tau_0}{\dot{\gamma}} \tag{2.16}$$

A relation analogous to the power law (Equation (2.8)) is derived from Equation (2.15) for $\tau > \tau_0$:

$$\eta = k \cdot \dot{\gamma}^{n-1}$$

2.1.1.3 Influence of Temperature and Pressure on the Flow Behavior

Factors determining the flow of melts besides shear rate $\dot{\gamma}$ and shear stress τ for a specific polymer melt are the melt temperature T, the hydrostatic pressure in the melt p_{hyd}, the molecular weight, and the molecular weight distribution, as well as additives, such as fillers and lubricants. For a given polymer formulation, the only free variables having an effect are $\dot{\gamma}$ or τ, p_{hyd}, and T.

Figure 2.8 (from [21]) illustrates a quantitative effect of the changes in temperature and pressure on the shear viscosity: an increase in pressure of approximately 550 bar for an observed sample of PMMA (polymethylmethacrylate) resulted in a tenfold increase in viscosity. Or, in order to keep viscosity constant, in this case the temperature would have to be increased by approximately 23 °C.

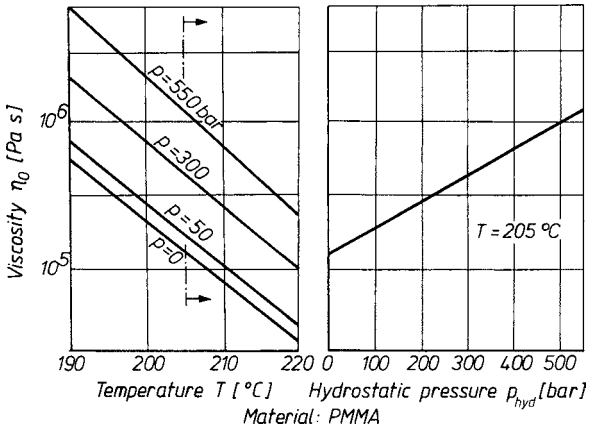

Figure 2.8 Viscosity as a function of temperature and of hydrostatic pressure (according to [21])

Figure 2.9 [22] provides a picture of the behavior of viscosity with the change of temperature for various polymers. It can be clearly seen that semicrystalline polymers, which have a low T_g when compared to amorphous polymers, exhibit a considerably lesser temperature dependence of their viscosity than the latter. This influence on the ability of polymers to flow can be essentially caused by two factors [23,24]:

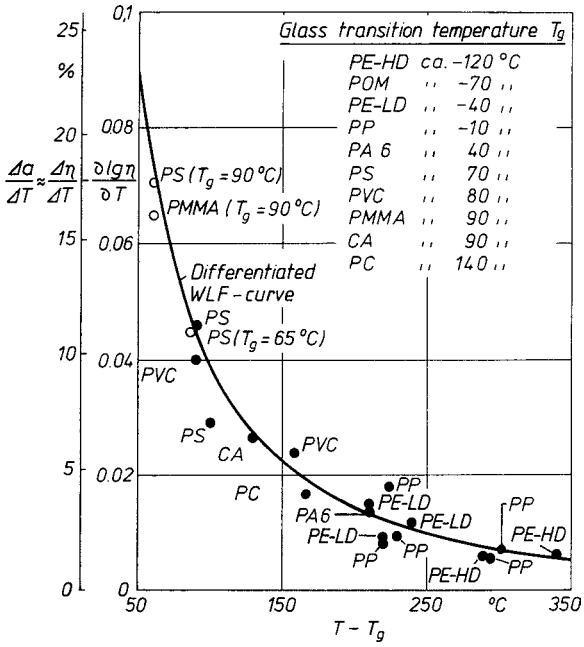

Figure 2.9 Change in viscosity with temperature for different polymers [22]

- A thermally activated process causing the mobility of segments of a macromolecular chain (i.e., the intramolecular mobility)
- The probability that there is enough free volume between the macromolecular chains allowing their place exchange to occur

The Influence of Temperature

When plotting viscosity curves at varied temperatures for identical polymer melts in a log-log graph (Fig. 2.10), the following can be established:

- First, the effect of temperature on the viscosity is considerably more pronounced at low shear rates, particularly in the range of the zero-shear viscosity, when compared to that at high shear rates.
- Second, the viscosity curves in the diagram are shifted with the temperature, but their shape remains the same.

It can be shown that for almost all polymeric melts (so-called thermorheologically simple fluids [25]) the viscosity curves can be transformed into a single master curve that is independent of temperature. This is done by dividing the viscosity by the temperature corresponding to η_0 and multiplying the shear rate with η_0 [1,2,25,26]. Graphically, this means that the curves are shifted along a straight line with a slope of –1, i.e., along a line $\log(\eta_0(T))$ to the right and simultaneously downward and thus transformed into a single curve (Fig. 2.10). This is referred to as the *time-temperature superposition principle.*

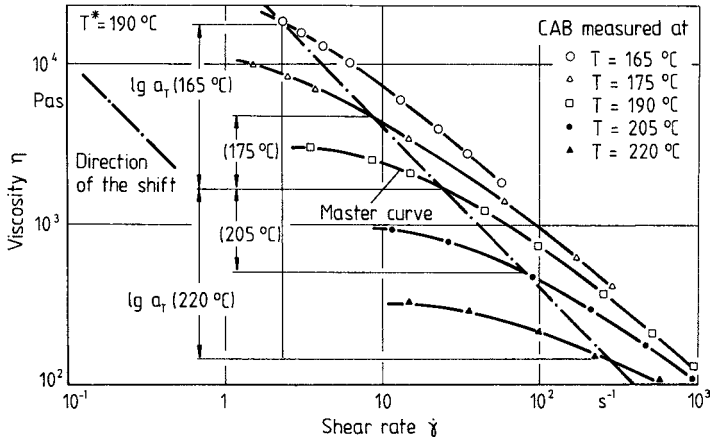

Figure 2.10 Viscosity curves for cellulose acetate butyrate (CAB) at various temperatures

This time-temperature superposition leads to the plotting of the reduced viscosity η/η_0 against $\eta_0\dot{\gamma}$. In this way a single characteristic function for the polymer is obtained:

$$\frac{\eta\left(\dot{\gamma},T\right)}{\eta_0\left(T\right)} = f\left(\eta_0\left(T\right)\cdot\dot{\gamma}\right). \tag{2.17}$$

Here, T as the reference temperature can be chosen freely.

When seeking the viscosity function for a certain temperature T with only the master curve or the viscosity curve at a certain other temperature T_0 given, a temperature shift is necessary to obtain the required function. First, it is not known how much the curve has to be shifted. The shift factor a_T required here can be found as follows:

$$a_T = \frac{\eta_0\left(T\right)}{\eta_0\left(T_0\right)} \quad \text{or} \quad \lg a_T = \lg\frac{\eta_0\left(T\right)}{\eta_0\left(T_0\right)}. \tag{2.18}$$

The quantity $\lg a_T$ is the distance that the viscosity curve at the reference temperature T_0 has to be shifted in the direction of the respective axes (Fig. 2.11).

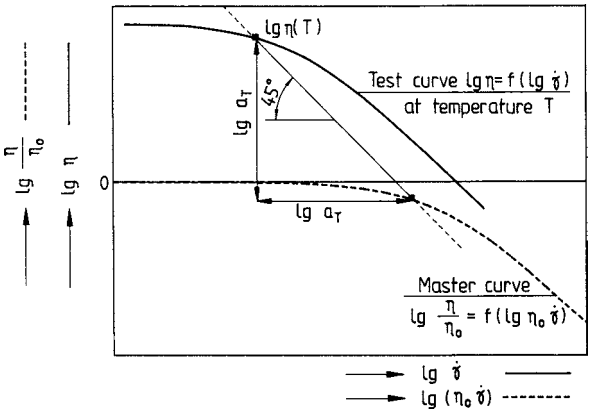

Figure 2.11 Time-temperature superposition principle for a viscosity function

There are several formulas for the calculation of the temperature shift factor. Two of them are the most important and should be mentioned, namely the Arrhenius law and the WLF equation.

The Arrhenius law can be derived from the study of a purely thermally activated process of the interchange of places of molecules:

$$\lg a_T = \lg \frac{\eta_0(T)}{\eta_0(T_0)} = \frac{E_0}{R}\left(\frac{1}{T} - \frac{1}{T_0}\right). \tag{2.19}$$

where E_0 is the flow activation energy in J/mol specific for the given material, and R is the universal gas constant equal to 8.314 J/(mol·K).

The Arrhenius law is suitable particularly for the description of the temperature dependence of the viscosity of semicrystalline thermoplastics [9,25].

For small temperature shifts or rough calculations, a_T can be approximated from an empirical formula, which is not physically proven and which takes the following form [1,9]:

$$\lg a_T = -\alpha \cdot (T - T_0) \tag{2.20}$$

where α is the temperature coefficient of viscosity specific to the given material.

Another approach based on the free volume, i.e., the probability of the place exchange, was developed by *Williams, Landel,* and *Ferry* [27]. It was originally applied to the temperature dependence of relaxation spectra and later was applied to viscosity. The relationship (also known as the WLF equation) in its most usual form is

$$\lg a_T = \lg \frac{\eta(T)}{\eta(T_S)} = -\frac{C_1 \cdot (T - T_S)}{C_2 + (T - T_S)}, \tag{2.21}$$

which relates the viscosity $\eta(T)$ at the desired temperature T to the viscosity $\eta(T_S)$ at the standard temperature T_S with shear stress being constant. For T_S equal approximately to $T_g + 50$ K [27] (i.e., 50 K above the glass transition temperature), $C_1 = -8.86$ and $C_2 = 101.6$ K.

The glass transition temperatures of several polymers are shown in Fig. 2.9, and additional values are in [28]. The measurement of T_g of amorphous polymers can be done in accordance with DIN EN ISO 75-2, Procedure A, which is a test for the deflection temperature of plastics under load; in the USA the corresponding ASTM standard is ASTM D 648 ISO 75. The softening temperature determined by this test can be set equal to T_g [7].

A more accurate description is possible when T_S (and, if necessary, C_1 and C_2, which also can be considered as almost material independent) is determined from regression of the viscosity curves, measured at different temperatures. Although the WLF equation pertains by definition to amorphous polymers only and is superior to the Arrhenius law [9,24,25], it still can be used for semicrystalline polymers with an acceptable accuracy [22,29–32].

Figure 2.12 compares the determination of the shift factor a_T obtained from the Arrhenius law to that from the WLF equation [30]. When operating within the temperature range ±30 K from the reference temperature, which is often sufficient for practical purposes, both relations are satisfactory.

There are basically two reasons for favoring the WLF equation, however:

- The standard temperature T_S is related to the known T_g for the given material with a high enough accuracy ($T_S \approx T_g + 50$ K).
- The effect of pressure on the viscosity can be easily determined when operating above the standard temperature (this will be explained further at a later point).

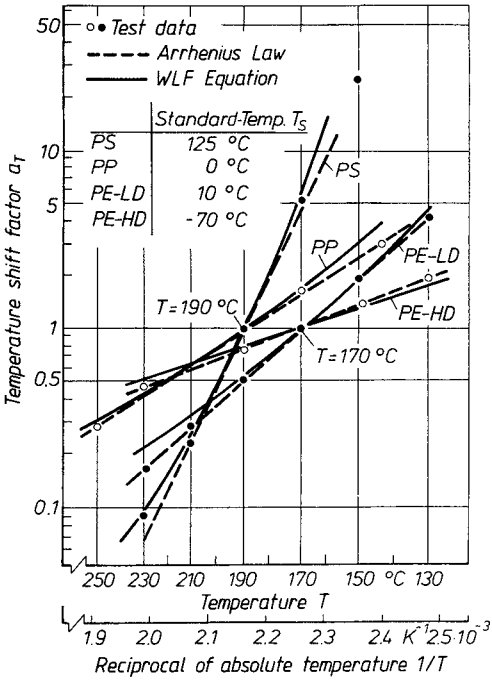

Figure 2.12 Temperature shift factor a_T for different polymers

When the shift of a viscosity curve from one arbitrary temperature T_0 to the desired temperature T is performed using the WLF equation, Equation (2.21) is used twofold:

$$\lg a_T = \lg \frac{\eta(T)}{\eta(T_0)} = \lg\left(\frac{\eta(T)}{\eta(T_S)} \cdot \frac{\eta(T_S)}{\eta(T_0)}\right) = \lg\left(\frac{\eta(T)}{\eta(T_S)}\right) + \lg\left(\frac{\eta(T_S)}{\eta(T_0)}\right) = \lg\left(\frac{\eta(T)}{\eta(T_S)}\right) - \lg\left(\frac{\eta(T_0)}{\eta(T_S)}\right) \quad (2.22)$$

$$= \frac{C_1(T_0 - T_S)}{C_2 + (T_0 - T_S)} - \frac{C_1(T - T_S)}{C_2 + (T - T_S)},$$

with $C_1 = 8.86$ and $C_2 = 101.6$ K, and T_0 is the reference temperature at which the viscosity is known.

The Influence of Pressure

The effect of pressure on the flow behavior can be determined along with the expression for the temperature dependence from the WLF equation [29]. It turns out that the standard temperature T_s, which lies at approximately $T_g + 50$ K, used in the WLF equation at 1 bar, increases with pressure. This shift corresponds in turn to the shift in T_g, which can be determined directly from a p-ν-T diagram [22,33].

The pressure dependence of the glass transition temperature can be assumed to be linear up to pressures of about 1000 bar (Fig. 2.13 [34]), thus:

$$T_g(p) = T_g(p = 1\,\text{bar}) + \xi \cdot p. \tag{2.23}$$

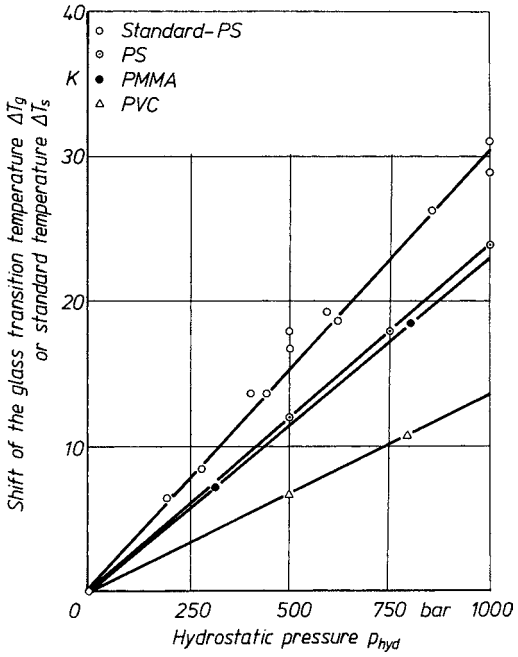

Figure 2.13 Effect of pressure on the glass transition and the standard temperature

The resulting shifts in T_g are of the order of 10 to 30 K per 1000 bar. At pressures higher than 1000 bar, the glass transition temperature increases with increasing pressure at a much smaller rate.

If there is no p-υ-T diagram available for the given polymer from which the pressure dependence of its T_g could be determined, it can be estimated by the following relation:

$$T_g \approx T_g(1\ \text{bar}) + (10 \text{ to } 30) \cdot 10^{-3}\ \text{K/bar} \cdot p \tag{2.24}$$

where p is the desired pressure in bar. (Generally, it is known that the pressure affects the flow properties of amorphous polymers stronger than the flow of semi-crystalline polymers.)

Then, the WLF shift from a viscosity curve at the temperature T_1 and the pressure p_1 to another one at T_2 and p_2 respectively can be performed. The shift factor a_T can be calculated as follows:

$$\begin{aligned} \lg a_T &= \lg \left(\frac{\eta\ (T_2, p_2)}{\eta\ (T_1, p_1)} \right) \\ &= \frac{C_1 \cdot (T_2 - T_S(p_2))}{C_2 + (T_2 - T_S(p_2))} - \frac{C_1 \cdot (T_1 - T_S(p_1))}{C_2 + (T_1 - T_S(p_1))}. \end{aligned} \tag{2.25}$$

of the resistance of the melt to elongational deformation. The inlet pressure loss can be taken into account by applying Equation (5.81) and subtracting this pressure loss from the driving pressure $\bar{p}$, thus:

$$\dot{V}_L = f\left[\left(\bar{p} - \Delta p_E - p_0\right), H(x), y(x)\right]. \tag{5.85}$$

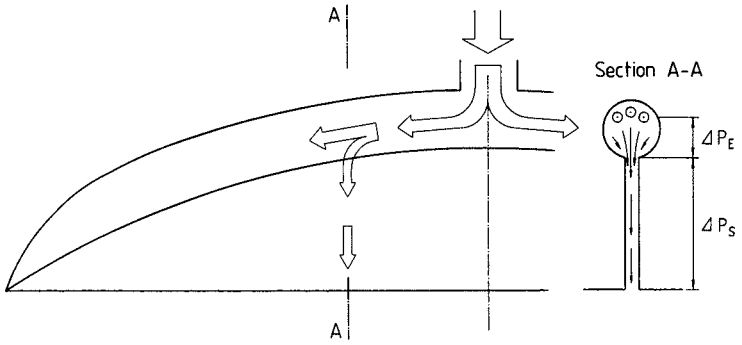

Figure 5.27 Inlet pressure drop due to the flow from the distribution channel into the land gap

The fact that the inlet pressure loss Δp_{entry} depends on the volumetric flow rate through the slit and the geometric conditions has to be considered:

$$\Delta p_{entry} = f\left[\dot{V}_L, H(x), R(x)\right]. \tag{5.86}$$

The disadvantages of the numerical design of the flow channel are as follows: a great deal of programming is necessary, the design requires long computing times, and mathematical stability problems frequently occur in many applications.

5.2.2.5 Considerations for Clam Shelling

So-called clam shelling (opening up) due to the existing internal pressures is one of the problems in the design of wide slit dies. The pressure distribution in a wide slit die is depicted schematically in Fig. 5.28. Figure 5.29 shows the resulting deformation of the die plates (see also Section 9.3 on this). The clam shelling increases the melt flow in the center region of the die.

The effect of this widening can be taken into account during the die design only when the magnitude of the deflection as a function of the pressure distribution can be determined. To compensate for the widening, the die can be made in such a way that if it widens during the operation, it has the computed flow channel geometry. This means that the die is made with a much smaller land slit in the middle region.

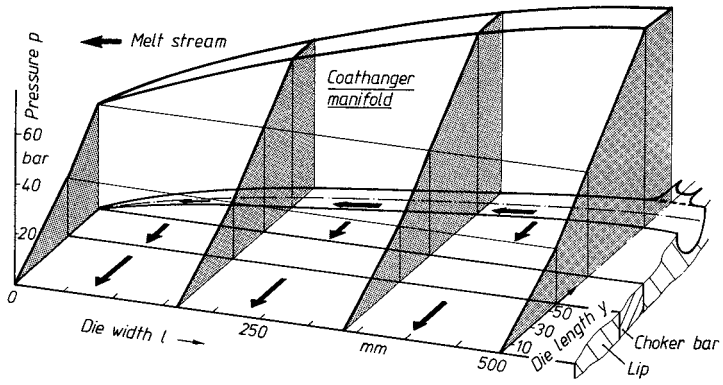

Figure 5.28 Typical pressure distribution in a flat slit die

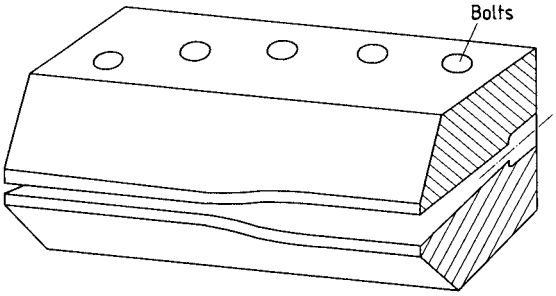

Figure 5.29 Clam shelling due to internal pressure in a flat slit die

Another possibility is to take the widening into account during the rheological design of the land length or of the contour of the distribution channel. This means that the manifold has to be designed with the height of the land slit changing across its width [70].

The possibilities of predicting the die widening by computation are discussed in Section 9.3 [77].

5.2.2.6 Unconventional Manifolds

Manifold systems that accomplish the melt distribution across a distribution channel and a land region are designed in such a way that for a uniform emerging flow there is an equal resistance to flow on each flow path. A situation where each flow path has equal flow history as to the residence time and shear action cannot be achieved by these systems (fishtail, coathanger). Therefore, alternatives have been recommended that are designed in such a way that each flow path is made the same length [78]. When observing the flow paths in a wide slit die (Fig. 5.30) that is made as a divergent slit channel with a constant slit height, it is obvious that the flow paths in the die center are shorter than those at its edges. Under the

assumption of a point-like melt feed, the following relationship for minimum and maximum length of flow are valid:

$$l_p(0) = y_0, \tag{5.87}$$

$$l_p(L) = \sqrt{y_0^2 + L^2}. \tag{5.88}$$

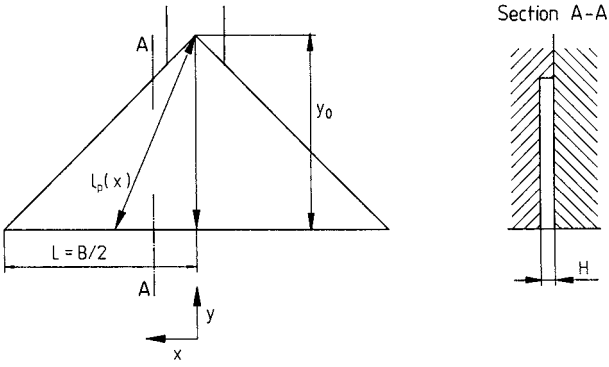

Figure 5.30 Streamlines in a divergent flow channel

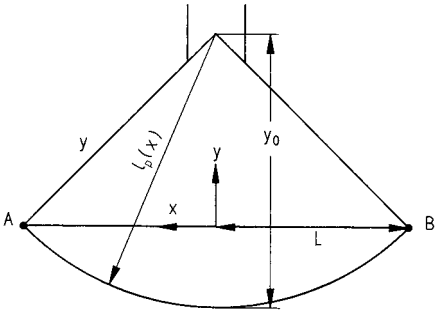

Figure 5.31 Streamlines in a centrally injected circular section

A flow channel geometry with equal lengths on each flow path can be derived from a study of a centrally injected circular sector (Fig. 5.31). In this case, all flow paths are equally long; however, the melt discharge is not located on the desired plane. This can be corrected by curving the circular sector in the third dimension (z direction) so that all flow paths end on the line A–B.

Such a manifold has been used successfully in injection molding as a predistributor for a film sprue [79].

In Fig. 5.32, there is a simple suggestion for the solution of the design of such a manifold. Each flow path is raised in the middle to such an extent ($h(x)$) that the length of the flow path ends on the edge of the die. The amount of elevation depends on the point of exit x. With the projected length of the flow path

$$l_p(x) = \sqrt{y_0^2 + x^2}, \tag{5.89}$$

the length of flow at the edge of the die

$$l_p(L) = \sqrt{y_0^2 + L^2} = l(x) \tag{5.90}$$

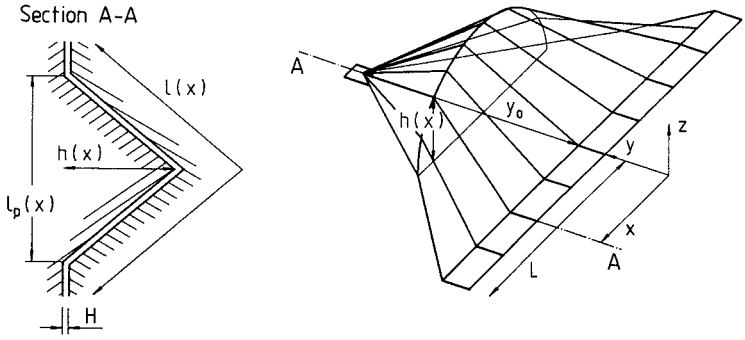

Figure 5.32 Flat slit manifold with streamlines of equal length

and the resulting length of the flow path

$$l(x) = 2\sqrt{\left(l_p(x)/2\right)^2 + h^2(x)} \tag{5.91}$$

the $h(x)$ for each flow path follows:

$$h(x) = \frac{1}{2}\sqrt{L^2 - x^2}. \tag{5.92}$$

It is important to keep in mind that all the quantities refer to the point of exit x. The above simple suggestion for a solution is not the optimum from the rheological point of view because of the sharp break in the flow path, but it still was chosen for the illustration of the process for the determination of the geometry for a wide slit die with flow paths of equal length.

The advantages are

- independence of the material being used,
- independence of operation conditions,
- uniform distribution, and
- identical flow history on each flow path.

Disadvantages of these dies are as follows:

- The die when built is rather high. For the type of adjustment of the flow path described above, the maximum height in the center of the die can be a quarter of the width of the exit slit. Therefore, the application of this principle is feasible for narrow dies only.
- Both halves of the die can be made only by CNC milling machines. Moreover, the machining times are long and the material consumption is very high because a great deal of it has to be machined away to produce a deep channel.
- The setting up of the control program for the CNC machines is very time consuming, considerably more so than that for conventional wide slit dies with a manifold.

5.2.2.7 Operating Performance of Wide Slit Dies

As explained earlier, it is possible to design extrusion dies with wide slit openings that are independent of the operating conditions. When the width of the die is more than 500 mm, the long lands resulting from the design procedure give rise to high pressure losses, which lead to high separating forces. These can be held back only by extremely thick die plates. Because of this limitation, the wide slit dies are in most cases designed as dependent on operating conditions.

Since these dies are operating under a variety of operating conditions and with a variety of materials, their process behavior, that is, the effect of changes in material and operating conditions on the melt distribution, is an important design criterion. A simple method to determine if the die is dependent on the process conditions is to do the design for a spectrum of operating conditions and then compare the resulting geometries (Fig. 5.33) [80].

The larger the change in the resulting geometry at various operating conditions, the more process-dependent the die is.

The procedure described above provides a reference point for the design, but an evaluation of the resulting melt distribution is not possible.

This evaluation is only possible after the computation of the effect of the operating point on the geometry of coathanger manifolds, designed to be independent of operating conditions [80] and die flow simulation [76,81–84].

For the above computation, the distribution channel is divided into segments, including the corresponding slit segments (Fig. 5.26). A flow and pressure balance is carried out successively for each segment. The procedure here is similar to the numerical design of the flow channel, the only difference being that in this case the geometry is fully specified and the exiting flow is calculated.

Index